

Nuclear magnetic resonance on oriented ¹⁰⁵Rh in Fe and Ni

E. Hagn and J. Wese*

Physik-Department, Technische Universität München, D-8046 Garching, Federal Republic of Germany.

G. Eska

Zentralinstitut für Tieftemperaturforschung, D-8046 Garching, Federal Republic of Germany

(Received 19 December 1980)

The magnetic hyperfine splitting frequencies $\nu_M = g\mu_N B_{HF}/h$ of ¹⁰⁵Rh ($j^\pi = 7/2^+$; $T_{1/2} = 35.4$ h) as dilute impurities in Fe and Ni have been measured with nuclear magnetic resonance on oriented nuclei as $\nu_M(^{105}\text{RhNi}) = 218.06(5)$ MHz and $\nu_M(^{105}\text{RhFe}) = 539.62(3)$ MHz. With the hyperfine field $B_{HF}(^{105}\text{RhFe}) = -556.6(1.2)$ kG the g factor of the ¹⁰⁵Rh ground state is derived as $|g| = 1.272(2)$. In combination with earlier nuclear orientation measurements $j^\pi = 7/2^{(+)}$ can be uniquely assigned. The g factor fits well into the systematics of $\pi g_{9/2}$ g factors in this mass region and confirms the interpretation of this state as $(\pi g_{9/2})_{7/2^+}^3$ shell model configuration. The hyperfine field of ¹⁰⁵RhNi is deduced as $-224.9(5)$ kG for $T = 0$ K. Hyperfine anomalies, the abnormal resonance shift with B_0 , and the overall systematics of $\pi g_{9/2}$ g factors are discussed.

[RADIOACTIVITY ¹⁰⁵Rh from ¹⁰⁴Ru(n, γ)¹⁰⁵Ru \rightarrow ¹⁰⁵Rh; NMR on oriented nuclei; deduced j, μ . Hyperfine fields, hyperfine anomaly. Knight shift.]

I. INTRODUCTION

In the odd Rh isotopes the energetically lowest states are expected to be single-particle states with configurations $(\pi g_{9/2})_{9/2^+}$ and $(\pi p_{1/2})_{1/2^-}$. In addition a $7/2^+$ state occurs (see Fig. 1), which decreases in energy from 201 keV in ⁹⁹Rh to 40 keV in ¹⁰³Rh, and which is the ground state of ¹⁰⁵Rh. These states have been interpreted as three-quasi-particle intruder states (configuration $(\pi g_{9/2})_{7/2^+}^3$).^{1,2} This assignment can be tested by a measurement of the nuclear g factors as then $g(7/2^+) = g(\pi g_{9/2})$ is expected.

The NMR-ON technique³ (nuclear magnetic resonance on oriented nuclei) is well suited for precise measurements on ¹⁰³Rh^m ($T_{1/2} = 56.1$ min; populated in the decay of ¹⁰³Pd) and ¹⁰⁵Rh ($T_{1/2} = 35.4$ h). We report here on NMR-ON measurements on ¹⁰⁵RhFe and ¹⁰⁵RhNi; a brief description has been given elsewhere.⁴ Meanwhile two NO-measurements on ¹⁰⁵RhFe have been reported,^{5,6} the results being in agreement with the NMR-ON data. A NMR-ON experiment on ¹⁰³Rh^mFe has also been published⁷; the g factor for the $7/2^+$ state deduced in this paper has, we think, to be reinterpreted as the used hyperfine field is in contradiction with all other data on RhFe and RhNi. This problem, which is connected with the abnormal resonance shift of ¹⁰³Rh^mFe, ¹⁰⁵RhFe, and ¹⁰⁵RhNi, will be discussed in detail. Further the hyperfine field for RhNi as determined in this work will be used for a more precise determination of the g factor of ¹⁰¹Rh^m ($j^\pi = 9/2^+$, $T_{1/2} = 4.4$ d) from the known NMR-ON frequency of ¹⁰¹Rh^mNi.⁸

II. EXPERIMENTAL PROCEDURE

A. NMR-ON method

The angular distribution of γ radiation emitted in the decay of oriented nuclei is given by⁹

$$W(\theta) = 1 + \sum_{k=2}^{k_{\max}} U_k F_k B_k(\mu B/kT) P_k(\cos\theta) Q_k. \quad (1)$$

Here the U_k are parameters describing the reorientation of the nucleus due to unobserved preceding decays; the F_k are the angular correlation coefficients for the observed γ transition; the P_k are the Legendre polynomials, θ representing the angle between the direction of γ -ray emission and the quantization axis (in the present case identical

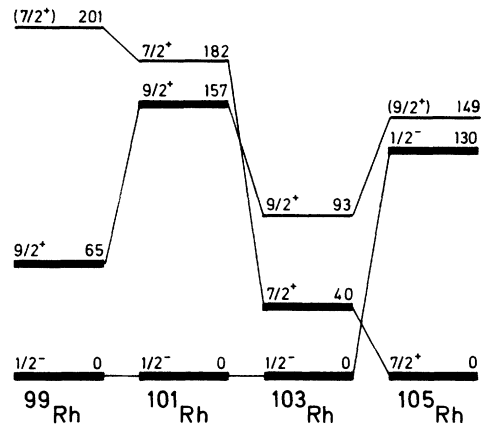


FIG. 1. Low-energy level schemes of ⁹⁹⁻¹⁰⁵Rh. The $7/2^+$ state, which becomes the ground state of ¹⁰⁵Rh, is believed to be a $(\pi g_{9/2})_{7/2^+}^3$ three-quasiparticle state.

with the direction of magnetization); and the Q_k are parameters correcting for the finite solid angle of the detector. The orientation of the initial state is described by the orientation parameters B_k , which are mainly functions on $\mu B/kT$ and which are nearly independent of the spin of the oriented state. Therefore the analysis of the temperature dependence of γ -anisotropies yields information on the magnetic moment μ of the oriented state.

The g factor of the oriented state can be determined with the technique of NMR on oriented nuclei.³ Here the γ anisotropy as given by Eq. (1) is used as detector for NMR. The resonance condition is given by

$$\begin{aligned} \nu &= \nu_M + b_s(1+K)B_0, \\ \nu_M &= |g \mu_N B_{HF} / h|, \\ b_s &= |g \cdot \mu_N / h| \text{sign}(B_{HF}). \end{aligned} \quad (2)$$

Here ν_M is the zero-field hyperfine splitting frequency; b_s is the resonance shift parameter as expected in the absence of a Knight shift; K is the Knight-shift parameter; and B_0 is the external magnetic field. A combination of NO and NMR-ON measurements yields μ and g ; in this way the spin of the oriented state can be determined.

B. Decay scheme of ^{105}Rh

A simplified decay scheme of ^{105}Rh is illustrated in Fig. 2. The $E2/M1$ mixing ratio δ of the 319-keV transition (absolute intensity 19.6%) has been determined as $+0.091(13)$ (Ref. 5) and $+0.11(1)$.⁶ The 319-keV γ anisotropy $W(\theta)-1$ at 10 mK for $\theta=0^\circ$ is ~ -0.40 and ~ -0.65 with Ni and Fe as host lattice, respectively, which is large enough for NMR-ON measurements.

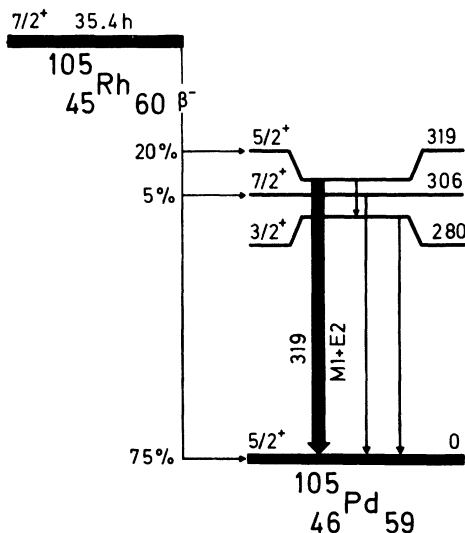


FIG. 2. Simplified decay scheme of ^{105}Rh .

III. SAMPLE PREPARATION AND LOW-TEMPERATURE APPARATUS

Samples of $^{105}\text{RhFe}$ and $^{105}\text{RhNi}$ were prepared in the following way: isotopically enriched ^{104}Ru ($>90\%$) was melted with highly pure Fe and Ni. Several melting steps were performed until the final concentration of ~ 0.1 at. % ^{104}Ru was reached. The alloys were coldrolled to a thickness of ~ 1 μm ; samples with an area of 8×8 mm^2 were then irradiated at the Forschungsreaktor in Karlsruhe (FR2) for ~ 3 d in a neutron flux of 10^{14} $n/\text{sec cm}^2$ in order to produce ^{105}Ru which decays to ^{105}Rh with a half-life of 4.4 h. After the irradiation the samples were annealed at $\sim 700^\circ\text{C}$ in a hydrogen atmosphere. Two samples were soldered to the Cu coldfinger of a single-stage demagnetization cryostat, details of which are described in Ref. 10. Using Cr-K-alum as cooling salt, final temperatures of ~ 10 mK were obtained. The samples were polarized with an external magnetic field $B_0 < 7$ kG which was provided by superconducting split coils. Perpendicular to B_0 the rf field was applied with a one-turn rf coil. The rf was frequency modulated with a modulation width $\Delta f = 0.1 \dots 2$ MHz and was swept continuously over the resonance region. Details of the rf electronics are given in Refs. 10 and 11. The γ radiation was detected with 4 7.5 $\text{cm} \times 7.5$ cm ϕ NaI(Tl) detectors, which were placed at 0° , 90° , 180° , and 270° with respect to B_0 . The γ counts of the 319-keV γ rays were selected with single-channel discriminators, accumulated in a multichannel analyzer, and recorded onto magnetic tape. The final analysis was performed at the Amdahl 470 computer of the IPP in Garching.

IV. RESULTS

A. $^{105}\text{RhNi}$

The resonance was searched between 150 and 250 MHz. Figure 3 shows a NMR-ON spectrum of the frequency region 212–228 MHz. There is obviously one resonance at 215.5(5) MHz. For the further measurements the frequency region was chosen smaller and the external field was varied. Figure 4 shows NMR-ON resonances measured for different values of B_0 . Here two successively measured spectra with opposite sweep direction were always added together. In this way the possible shift of the resonance center in sweep direction due to the finite spin lattice relaxation time is compensated. Such shifts have been observed¹¹ if the time interval during which the resonance region is passed is of the order of the spin-lattice relaxation time. Here the sweep rate for the rf has been chosen so small that no

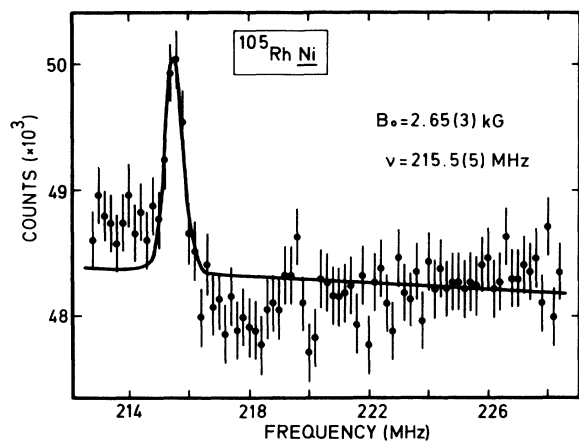


FIG. 3. NMR-ON resonance of $^{105}\text{RhNi}$. The slightly higher background at the left side of the resonance is due to a frequency-dependent nonresonant rf-eddy-current heating.

time-dependent analysis of the resonance spectra is necessary. Figure 5 shows the resonance centers versus B_0 . The solid line is the result of a least-squares fit which yields

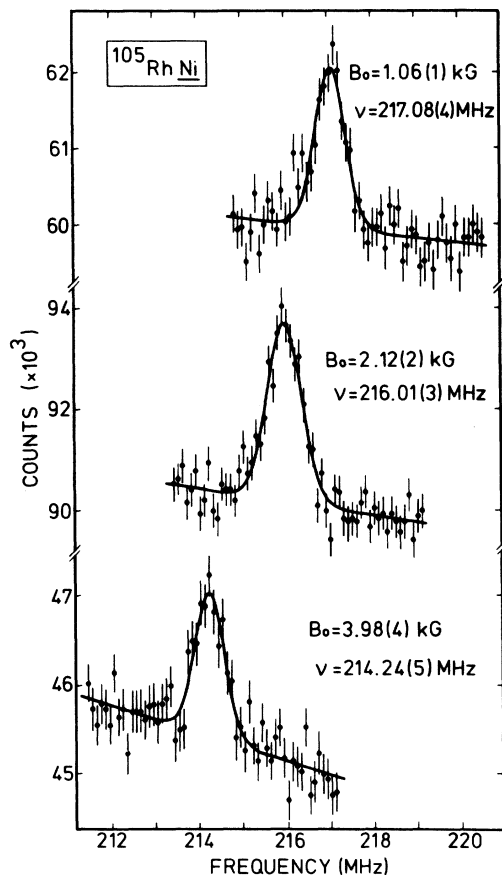


FIG. 4. NMR-ON resonances of $^{105}\text{RhNi}$ measured at $\theta = 0^\circ$ with respect to B_0 at a temperature of ~ 10 mK.

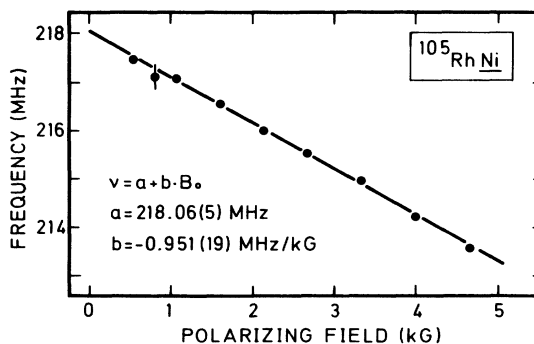


FIG. 5. $^{105}\text{RhNi}$ resonance shift with the external magnetic field.

$$\nu(B_0 = 0) = 218.06(5) \text{ MHz},$$

$$d\nu/dB_0 = -0.951(19) \text{ MHz/kG}.$$

B. $^{105}\text{RhFe}$

Taking into account the expected ratio for the hyperfine fields of Rh in Ni and Fe the resonance was searched between 526 and 553 MHz. Figure 6 shows NMR-ON spectra measured for $B_0 = 1.06(1)$, $3.18(3)$, and $5.31(5)$ kG. Similar measurements were performed for a total of 17 values for the external magnetic field up to $6.46(6)$ kG. Figure 7 shows the resonance centers versus B_0 . The least-squares fit yields

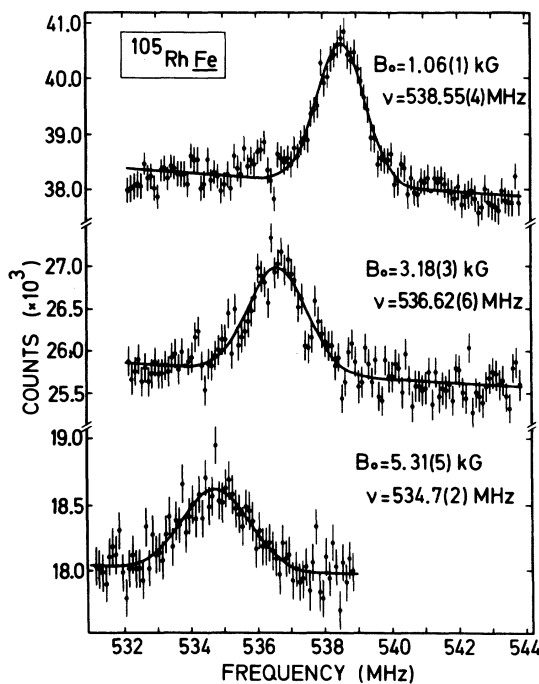


FIG. 6. NMR-ON resonances of $^{105}\text{RhFe}$. The increase of the line width with B_0 may be due to a non-complete alignment of the hyperfine field.

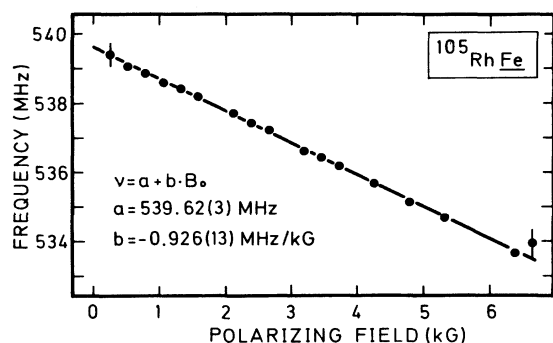


FIG. 7. $^{105}\text{RhFe}$ resonance shift with the external magnetic field.

$$\nu(B_0 = 0) = 539.62(3) \text{ MHz},$$

$$d\nu/dB_0 = -0.926(13) \text{ MHz/kG}.$$

V. DISCUSSION

A. Hyperfine fields of RhFe and RhNi

The essential point for the derivation of nuclear g factors from measured hyperfine frequencies is the use of correct and appropriate values for the respective hyperfine fields. As the tabulated values¹² for B_{HF} (RhFe) and B_{HF} (RhNi) do not represent the actual revision state we will present the corresponding derivation here.

The hyperfine field is normally deduced from measured hyperfine splittings of nuclear states for which the g factor is known precisely. As B_{HF} depends on the temperature and (for some impur-

ity-host combinations) on the impurity concentration, the functional dependence on these parameters has to be taken into account. Moreover, the existence of hyperfine anomalies must not be neglected without an estimate of the respective correction factor.

In Table I we have listed experimentally known hyperfine splittings of ^{100}Rh ($E = 74.8 \text{ keV}$; $j^\pi = 2^+$; $T_{1/2} = 214 \text{ nsec}$), and ^{103}Rh (g.s., $j^\pi = \frac{1}{2}^-$) in Fe and Ni. The hyperfine fields have been deduced using the relation

$$\nu(\text{MHz}) = 0.762 \ 2532 \times B_{\text{HF}}(\text{kG}) \times g.$$

At a first view the low-temperature results for $^{100}\text{RhFe}$ ($B_{\text{HF}} = -556.5(1.2) \text{ kG}$) and $^{103}\text{RhFe}$ ($B_{\text{HF}} = -536.86(12) \text{ kG}$) seem to be contradictory. As already pointed out by Matthias *et al.*¹³ the different results can be explained by hyperfine anomaly²³; because of their different distributions over the finite size of the nucleus, the spin and orbital parts of the nuclear magnetic moment experience different magnetic fields from the contact part of the magnetic hyperfine interaction if the atomic number is large enough that the contact field varies considerably over the nuclear volume. Thus the average field sensed by the moment depends on the nucleon distribution

$$\mu B^{\text{eff}} = \int \mu(r) B(r) dr = \mu B(0) \cdot (1 + \epsilon). \quad (3)$$

Here ϵ describes the deviation from the point-dipole interaction, it depends on the wave function of the nuclear state. This effect causes the ratio

TABLE I. Hyperfine splittings and hyperfine fields of Rh isotopes in Fe and Ni.

Host	Isotope	j^π	g	Method	T (K)	c (at.%)	ν (MHz)	B_{HF} (kG)	Ref.
Fe	^{100}Rh	2^+	2.162(4) ^a	NMR/PAC	300	t	881.7(1.0)	535.0(1.2)	13
				NMR/PAC	77		912.5(1.0)	553.7(1.2)	
				NMR/PAC	0			556.5(1.2) ^b	
	^{103}Rh	$\frac{1}{2}^-$	0.1768(4) ^c	NMR	4.2	<2		-540(10) ^d	14
				NMR	1.4	2	72.4 ^e	15	
				NMR	1.4	3	72.4 ^e		
			NMR	1.6-4.2	3	72.5 ^f	16		
			NMR	4.2	0.48	72.35(2)	-536.86(12)	17	
Ni	^{100}Rh	2^+	2.162(4) ^a	NMR/PAC	296	t	337.8(4)	(-)205.6	18
				TDPAC	296	t	339.5(3)		
				TDPAC	77	t			
	^{105}Rh	$\frac{7}{2}^+$	1.272(2) ^h	NMR/ON	0	0.1	218.06(5)	-224.9(5)	h

^a Reference 20. [Recalculation of the original g factor, $g = 2.151(4)$ (Ref. 21), with the diamagnetic correction of Ref. 22.]

^b Extrapolated value.

^c Reference 20.

^d Recalculated; originally the authors used $\mu = -0.0879 \mu_N$.

^e Center of the main resonance.

^f Center of the main resonance; used for relaxation studies.

^g Recalculated; originally the authors used $g = 2.151$.

^h This work.

of the magnetic hyperfine splitting constants of two nuclear states in the same atomic environment to be different from the ratio of the respective g factors. The hyperfine anomaly (HA) is defined by the relation

$$\frac{\nu_1}{\nu_2} = \frac{g_1}{g_2} (1 + {}^1\Delta^2) \quad (4)$$

and can be expressed by

$${}^1\Delta^2 = \frac{\epsilon_1 - \epsilon_2}{1 + \epsilon_2} \approx \epsilon_1 - \epsilon_2. \quad (5)$$

The ratio of effective fields is given by

$$\frac{B_1^{\text{eff}}}{B_2^{\text{eff}}} = 1 + {}^1\Delta^2. \quad (6)$$

A calculation of the single-level anomalies ϵ according to Eisinger and Jaccarino²⁴ yields $\epsilon(^{100}\text{Rh}) = -0.46\%$, $\epsilon(^{103}\text{Rh}) = -4.2\%$, and $\epsilon(^{105}\text{Rh}) = -0.44\%$. The calculation for ^{100}Rh has been performed using the relation

$$\epsilon = \alpha_p \cdot \epsilon_p + \alpha_n \epsilon_n, \quad (7)$$

where α_p and α_n are the fractional contributions of the proton and neutron to the magnetic moment of ^{100}Rh and ϵ_p and ϵ_n are the values of the individual isotope single-level anomaly for the proton and neutron alone. The values for α_p and α_n have been estimated from the known configuration of the 2^+ state [$\alpha | (\pi g_{9/2})_{9/2} (\nu d_{5/2})_{5/2} >_{2^+} + \beta | (\pi g_{9/2})_{7/2}^3 \times (\nu d_{5/2})_{5/2} >_{2^+}$ (Ref. 25)] as $\alpha_p = 0.95 \pm 0.05$ and $\alpha_n = 0.05 \pm 0.05$.

The HA's are then found to be ${}^{100}\Delta^{103} = +3.7\%$ and ${}^{100}\Delta^{105} = -0.02\%$. The first value is in good agreement with the experimental ${}^{100}\Delta_{\text{exp}}^{103} = +3.65(15)\%$ as obtained using Eq. (6). The small HA between ^{100}Rh and ^{105}Rh is due to the fact that the main contribution to the magnetic moment of the 2^+ state in ^{100}Rh originates from the $g_{9/2}$ protons. Thus the effective hyperfine field for $^{105}\text{RhFe}$ at $T=0$ K is deduced as

$$B_{\text{HF}}(^{105}\text{RhFe}) = 556.6(1.2) \text{ kG}.$$

Taking now $\nu_M(^{105}\text{RhFe})/\nu_M(^{105}\text{RhNi}) = 2.4745(4)$ the hyperfine field for $^{105}\text{RhNi}$ at $T=0$ K is derived as

$$B_{\text{HF}}(^{105}\text{RhNi}) = -224.9(5) \text{ kG}.$$

The hyperfine field of $^{100}\text{RhNi}$ has been studied up to now only at 77 K and at higher temperatures.^{18,19} It was found that the temperature dependence of the reduced hyperfine field $H(T)/H(0)$ follows closely that of the reduced bulk magnetization of nickel metal.¹⁹ The bulk magnetization of nickel changes by only 0.5% between 77 and 0 K.²⁶ If the same change for the hyperfine field is assumed an extrapolated value for $T=0$ K of $-221(3)$

kG is obtained, which is in good agreement with the more precise value on $^{105}\text{RhNi}$.

B. Resonance shift

From the measured resonance shift $d\nu/dB_0$ we derive according to Eq. (2) $g(1+K) = 1.24(3)$ and $1.21(2)$ for $^{105}\text{RhNi}$ and $^{105}\text{RhFe}$, respectively. Taking $g = 1.272(2)$ (see Table II) we get $K(^{105}\text{RhNi}) = -2.5(2.5)\%$ and $K(^{105}\text{RhFe}) = -4.8(1.5)\%$. This holds with the assumption of $K(^{60}\text{CoFe}) = 0$ as we have calibrated the polarization field by measuring the resonance shift of $^{60}\text{CoFe}$ [$g(^{60}\text{Co}) = 0.7598$],²⁰ which was found to be reproducible within an accuracy of $\sim 1\%$. The assumption $K = 0$ was supported by the results of Mössbauer effect measurements on $^{57}\text{FeFe}$ in external fields up to 100 kG,²⁷ $K = -0.2(9)\%$. From ME-NMR measurements on $^{57}\text{CoFe}$ $K(^{57}\text{CoFe}) = +2.9(1.2)\%$ has been reported.²⁸ Taking this into account $K(^{105}\text{RhNi}) = -5.4(2.8)\%$ and $K(^{105}\text{RhFe}) = -7.7(2.0)\%$ would be obtained. From a NMR-ON measurement on $^{103}\text{Rh}^m\text{Fe}$ Kempter and Klein⁷ found $\nu(B_0=0) = 550.3(5)$ MHz and $d\nu/dB_0 = -0.933(17)$ MHz/kG. Taking $B_{\text{HF}} = -556.6(1.2)$ kG (for the hyperfine anomaly $|{}^{103m}\Delta^{105}| < 10^{-4}$ is expected as both states have the same configuration), $g = 1.297(3)$ and hence $K = -5.6(1.7)\%$ is found, which is in agreement with the present result.

Kempter and Klein discussed several effects which could cause a similar behavior in the Knight shift. Finally they assumed $K = 0$ and derived the g factor from the resonance shift as $g = 1.22(2)$, the resulting value for the hyperfine field $B_{\text{HF}} = -590(10)$ kG being totally inconsistent with all other experimental data (see Table I). They argued that a concentration dependence of B_{HF} could be (partly) responsible for this difference. NMR experiments on $^{103}\text{RhFe}$ performed for Rh concentrations down to 0.48 at.%^{15,17} have shown, however, that the maximum resonance signal at 72.4 MHz (see Table I) is not shifted in the concentration range $0 < c < 3$ at.%. This indicates that the $K = 0$ assumption is not justified, and that $K \sim -5\%$ has to be taken as an experimental fact with an unknown origin at present.

In the mass region $A > 90$ several different impurity-host combinations have been investigated with the NMR-ON method: $^{90,92}\text{Nb}^m\text{Fe}$,²⁹ $^{93}\text{Mo}^m\text{Fe}$,³⁰ $^{93,94,95}\text{TcFe}$,³¹ and $^{97}\text{RuFe}$.¹¹ In the cases of NbFe , MoFe , and RuFe the results are consistent with $|K| < 1\%$. The hyperfine field and the nuclear g factors as derived for $^{93,94,95}\text{TcFe}$ with the assumption of $K = 0$ fit well into the respective systematics, although the latter should not be overinterpreted. Thus RhFe seems to be an exceptional case. On the other hand, the derivation of reliable K values from the resonance shift of NMR-ON

TABLE II. g factors of Rh isotopes.

Isotope	j^π	E (keV)	g factor	Host	Hyperfine splitting	
					ν_M (MHz)	B_{HF} (kG)
^{101}Rh	$\frac{9}{2}^+$	157	1.208(4)	Ni	207.1(5) ^a	-224.9(5)
^{103}Rh	$\frac{7}{2}^+$	40	1.297(3)	Fe	550.3(5) ^b	-556.6(1.2)
	$\frac{9}{2}^+$	93	1.23(17) ^c			
^{105}Rh	$\frac{7}{2}^+$	0	1.272(2)	Fe	539.62(3) ^d	-556.6(1.2)

^a Reference 8.^b Reference 6.^c Reference 20.^d This work.

resonances may be complicated by "hidden" effects connected with the inhomogeneous linewidth. In the case of IrNi the anomalously high resonance shift ($K \sim +15\%$) (Ref. 32) could be explained by the observed fact that the main part of the experimental linewidth was due to quadrupole interaction, and that the relative amplitudes of the quadrupole subresonances change with the external field.¹⁰ In this way an additional shift of the effective center of an unresolved resonance spectrum may be introduced, thus simulating an abnormal Knight shift. In the present experiment the inhomogeneous linewidth was $\Gamma \sim 1.0$ MHz. (The difference to the observed linewidth of $\Gamma \sim 1.5$ MHz is due to the frequency modulation of the rf field.) With the use of more dilute samples it should be possible to reduce Γ significantly.¹⁰ A change of the structure of the resonance spectrum could then be observed more easily. Such experiments should be performed in order to investigate whether the observed shift is a real Knight shift.

C. Nuclear g factors

All currently known g factors of $\pi g_{9/2}$ and $(\pi g_{9/2})_{7/2}^3$ states of Rh isotopes are listed in Table II, together with the corresponding hyperfine splitting and the hyperfine field used for the derivation. From NO measurements on $^{105}\text{RhFe}$ Barclay *et al.*⁵ and Wittkemper *et al.*⁶ have determined the hyperfine splitting of $^{105}\text{RhFe}$ as 561(19) and 534(10) MHz. As the NO technique is sensitive essentially on μB and not on gB the good agreement with the present result can be interpreted as confirmation of the correct spin assignment $j^\pi = \frac{7}{2}^{(*)}$. Thus we can use our g factor

$$g(^{105}\text{Rh}) = 1.272(2)$$

to derive a final value of the magnetic moment

$$\mu(^{105}\text{Rh}) = 4.452(9) \mu_N.$$

In Fig. 8 the currently known g factors of $1\pi g_{9/2}^+$ states (circles), $(1\pi g_{9/2})_{8^+}^2$ states (squares), and $(1\pi g_{9/2})_{7/2}^3$ states (triangles) are plotted versus the proton number. Each of the points is labeled with the neutron number of the state involved. The main deviation of nuclear moments from the single-particle Schmidt value [$g_{sp}(\pi g_{9/2}) = 1.509$] is normally ascribed to first-order core polarization³³ and the anomalous orbital magnetism due to mesonic space-exchange currents.³⁴ While the first effect is state dependent, the second effect

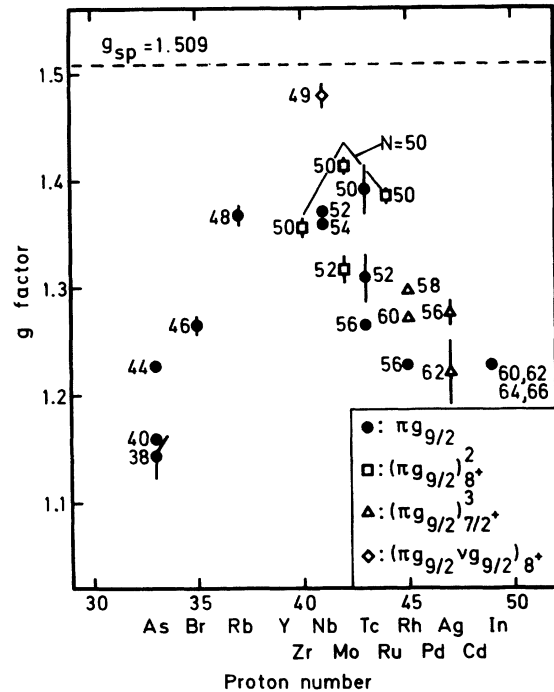


FIG. 8. g factors of $(\pi g_{9/2})_{9/2}^+$, $(\pi g_{9/2})_{8^+}^2$, and $(\pi g_{9/2})_{7/2}^3$ proton states as a function of the proton number. The respective neutron number is given beside each point. The solid line represents calculations of Häusser *et al.* (Ref. 35) for $N=50$ isotones. Contrary to the expectation the $\frac{7}{2}^+$ g factors are slightly larger than expected from the main trend of the $\frac{9}{2}^+$ g factors.

causes a state-independent deviation ($\delta g_1 \sim 0.1$). The main structure of Fig. 8 is thus due to core polarization. The increase of g between $Z=30$ and 40 is due to the successive filling of the $\pi f_{5/2}$ and $\pi p_{1/2}$ shells by which the $\pi f_{7/2} \rightarrow \pi f_{5/2}$ and $\pi p_{3/2} \rightarrow \pi p_{1/2}$ core polarization is blocked. The decrease of g for $Z > 40$ is due to the successive filling of the $\pi g_{9/2}$ shell by which the $\pi g_{9/2} \rightarrow \pi g_{7/2}$ core polarization can be active. The maximum g factor is thus expected for a $Z=40$ core. The solid line in Fig. 8 is the result of calculations for $N=50$ isotones of Häusser *et al.*³⁵; taking into account the mesonic current, the experimental data for $N=50$ are well described. The general trend of g with increasing neutron number N is given by an increase of g for $Z < 40$ and a decrease of g for $Z > 40$. Only Rh seems to be an exceptional case, as g for $^{101}\text{Rh}^m$ is smaller than g of $^{103}\text{Rh}^m$ and ^{105}Rh . On the other hand, the respective nuclear states

are different, as the configuration for $^{101}\text{Rh}^m$ is $(\pi g_{9/2})_{9/2}^+$ while it is (believed to be) $(\pi g_{9/2})_{7/2}^+$ for $^{103}\text{Rh}^m$ and ^{105}Rh . The g factors of the $\frac{7}{2}^+$ states in the neighbored Ag isotopes are also slightly higher than expected for $\frac{9}{2}^+$ states. According to the theoretical predictions of Kuriyama *et al.*³⁶ $g(\frac{7}{2}^+) < g(\frac{9}{2}^+)$ would be expected, which is not supported by the experimental data. Before final conclusions can be drawn further investigations are necessary, both experimentally and theoretically.

The authors are indebted to Professor P. Kienle for his continuous interest and support of this work. We also want to thank Dr. E. Zech for discussions and E. Smolic for his help with the cryostat. This work was supported by the Bundesministerium für Forschung und Technologie, Bonn and, in part, by the Kernforschungszentrum Karlsruhe.

* Present address: Lehrstuhl für Leichtbau, Technische Universität München, Arcisstr. 21, D-8000 München 2, Federal Republic of Germany.

¹L. S. Kisslinger, Nucl. Phys. **78**, 341 (1966).

²A. I. Sherwood and A. Goswami, Nucl. Phys. **89**, 465 (1966).

³E. Matthias and R. J. Holliday, Phys. Rev. Lett. **17**, 897 (1966).

⁴J. Wese, E. Hagn, P. Kienle, and G. Eska, in *Proceedings of the International Conference on Hyperfine Interactions Studied in Nuclear Reactions and Decay, Uppsala, Sweden, 1974*, edited by E. Karlsson and R. Wäppling (Uplands Grafiska AB, Uppsala, 1974), p. 112.

⁵J. A. Barclay, S. S. Rosenblum, W. A. Steyert, and K. S. Krane, Phys. Rev. C **14**, 1183 (1976).

⁶G. Wittkemper, H. D. Rüter, W. Haaks, and E. Gerdau, Hyp. Int. **3**, 157 (1977).

⁷H. Kempter and E. Klein, Z. Phys. A **281**, 341 (1977).

⁸G. Kaindl, F. Bacon, H.-E. Mahnke, and D. A. Shirley, Phys. Rev. C **8**, 1074 (1973).

⁹S. R. de Groot, H. A. Tolhoek, and W. J. Huiskamp, in *Alpha, Beta, and Gamma Ray Spectroscopy*, edited by K. Stegbahn (North-Holland, Amsterdam, 1968), Vol. 2, p. 1199.

¹⁰E. Hagn, K. Leuthold, E. Zech, and H. Ernst, Z. Phys. A **295**, 385 (1980).

¹¹K. Leuthold, E. Hagn, H. Ernst, and E. Zech, Phys. Rev. C **21**, 2581 (1980).

¹²G. N. Rao, Hyp. Int. **7**, 141 (1979).

¹³E. Matthias, D. A. Shirley, N. Edelstein, H. J. Körner, and B. A. Olsen, in *Hyperfine Structure and Nuclear Radiations*, edited by E. Matthias and D. A. Shirley (North-Holland, Amsterdam, 1968), p. 878.

¹⁴M. Kontani and J. Itoh, J. Phys. Soc. Jpn. **22**, 345 (1967).

¹⁵M. Kontani, M. Ota, and Y. Masuda, J. Phys. Soc. Jpn. **29**, 1194 (1970).

¹⁶M. Kontani, T. Hioki, and Y. Masuda, J. Phys. Soc. Jpn. **32**, 416 (1972).

¹⁷R. H. Dean and G. A. Jakins, J. Phys. F **8**, 1563 (1978).

¹⁸S. Koicki, T. A. Koster, R. Pollak, D. Quitmann, and D. A. Shirley, Phys. Lett. **32B**, 351 (1970).

¹⁹R. C. Reno and C. Hohenemser, in *Hyperfine Interactions in Excited Nuclei*, edited by G. Goldring and R. Kalish (Gordon and Breach, New York, 1971), Vol. 2, p. 457.

²⁰*Table of Isotopes*, edited by C. M. Lederer and V. S. Shirley, 7th ed. (Wiley, New York, 1978), Appendix VII, p. A-42.

²¹E. Matthias and D. A. Shirley, Nucl. Instrum. Methods **45**, 309 (1966).

²²F. D. Feiock and W. R. Johnson, Phys. Rev. **187**, 39 (1969).

²³A. Bohr and V. F. Weisskopf, Phys. Rev. **77**, 94 (1950).

²⁴J. Eisinger and V. Jaccarino, Rev. Mod. Phys. **30**, 528 (1958).

²⁵E. Matthias, D. A. Shirley, J. S. Evans, and R. A. Naumann, Phys. Rev. **140**, B264 (1965).

²⁶B. E. Argyle, S. Charap, and E. W. Pugh, Phys. Rev. **132**, 2051 (1963).

²⁷S. Foner, A. J. Freeman, N. A. Blum, R. B. Frankel, E. J. McNiff, Jr., and H. C. Praddaude, Phys. Rev. **181**, 863 (1969).

²⁸R. Laurenz, E. Klein, and W. D. Brewer, Z. Phys. **270**, 233 (1974).

²⁹E. Hagn, E. Zech, and G. Eska (unpublished).

³⁰E. Hagn, E. Zech, and G. Eska, Phys. Rev. C **23**, 2252 (1981).

³¹E. Hagn, E. Zech, and G. Eska, Nucl. Phys. **A361**, 355 (1981).

³²E. Hagn and G. Eska, in *Proceedings of the International Conference on Hyperfine Interactions Studied in Nuclear Reactions and Decay, Uppsala, Sweden, 1974*, edited by E. Karlsson and R. Wäppling (Uplands Grafiska AB, Uppsala, 1974), p. 148.

³³A. Arima and H. Horie, Prog. Theor. Phys. **12**, 623 (1954).

³⁴T. Yamazaki, T. Nomura, S. Nagamiya, and T. Katou,
Phys. Rev. Lett. 25, 547 (1970).

³⁵O. Häusser, I. S. Towner, T. Faestermann, H. R.
Andrews, J. R. Beene, D. Horn, D. Ward, and

C. Broude, Nucl. Phys. A293, 248 (1977).

³⁶A. Kuriyama, T. Marumori, and K. Matsuyanagi,
Prog. Theor. Phys. 51, 779 (1974).